ACCURACY EVALUATION OF COASTLINE EXTRACTION METHODS IN REMOTE SENSING: A SMART PROCEDURE FOR SENTINEL-2 IMAGES

E. Alcaras [1], P. P. Amoroso [1], F. G. Figliomeni [1], C. Parente [2] *, G. Prezioso [2]

[1] International PhD Programme "Environment, Resources and Sustainable Development", Department of Science and Technology, Parthenope University of Naples, Centro Direzionale, Isola C4, (80143) Naples, Italy – (emanuele.alcaras, pierpaolo.amoroso, francescogiuseppe.figliomeni001)@studenti.uniparthenope.it
[2] Department of Science and Technology, Parthenope University of Naples, Centro Direzionale, Isola C4, (80143) Naples, Italy - (claudio.parente, pina.prezioso)@uniparthenope.it;

KEY WORDS: Unsupervised classification, K-Means, Sentinel-2, Coastline Extraction, GIS, DEM.

ABSTRACT:

Different algorithms are available in literature to extract coastline from remotely sensed images and different approaches can be adopted to evaluate the result accuracy. In every case, a reference coastline is suitable to compare alternative solutions: usually, the visual photointerpretation on the RGB composition of the considered imagery and the manually vectorization of the coastline allow an accurate term of comparison, but they are laborious and time consuming. This article aims to demonstrate that a smart procedure is possible using a LiDAR-generated Digital Elevation Model (Lg-DEM) as a useful source from which to rapidly extract the reference coastline. The experiments are carried out on Sentinel-2 imagery, using six indices: Normalized Difference Vegetation Index (NDVI), Normalized Difference Water Index (NDWI), Modified Normalized Difference Water Index (MNDWI), Enhanced Vegetation Index (EVI), Red-Green Ratio (RGR) and NIR-Red Ratio (NRR). The unsupervised classification algorithm named K-Means transforms each index resulting product in two clusters, i.e. water and no-water, while the automatic vectorization allows to detect the coastline as separation between land and sea. The coastline from Lg-DEM and the manually achieved one using photointerpretation are both assumed as references for testing result accuracy. In every case, the performance analysis of the six indices products induces similar results, confirming the combination of NDWI and K-Means as the most performing approach. The tests demonstrate that, when Lg-DEM and satellite images concern the same area in the same period or in absence of variations, the coastline extracted from Lg-DEM is useful as reference to compare various methods.

1. INTRODUCTION

Defined as the element of separation between land and sea (Dolan et al., 1980) (Specht et al., 2020), the coastline is of fundamental importance in many fields such as cartography (Fabris, 2021), coastal geomorphology monitoring (Palazzo et al., 2012) (Darwish et al., 2017) and maritime navigation (Bo et al., 2001). Due to the dynamics in place that can modify its shape and position (Prasad and Kumar, 2014), the coastline requires careful monitoring to identify its transformations. Since the on-site survey is expensive and time consuming (Nahon et al., 2019) and sometimes difficult to carry out due to the morphology of the places, remote sensing techniques are a valid alternative.

The processing of remote sensed images allows to derive the coastline in automatic way: this result can be achieved through supervised (Goksel et al., 2019) and unsupervised classification methods (Viana et al., 2019), or through suitable indices (Karaman, 2021). Supervised classification provides usually better results than unsupervised, but requires longer times and a greater expenditure of resources (Pawluszek-Filipiak and Borkowski, 2020). In fact, supervised techniques need some prior knowledge of samples of the image classes for training the program into the identification of the classes (Sisodia et al., 2014). However, in the literature it has been shown that unsupervised techniques can give excellent results if applied appropriately, i.e. on the map resulting from the application of the Normalized Difference Water Index (NDWI) (Alcaras et al., 2021a).

In any way, the result accuracy depends on many factors, i.e. applied method, sensor characteristics, coastline typology. In order to establish the effectiveness of a method in relation to these factors, a reference coastline to be compared with the automatically extracted one is necessary (Liu et al., 2017). Typically, we use the manually achieved shoreline from the panchromatic image (if available) or from the RGB composition as element of comparison. However, another important source for obtaining reference coastline is Digital Elevation Model (DEM). There are several techniques to acquire data for DEM generation, e.g. Airborne Light Detection and Ranging (LiDAR) (Chen et al., 2017) (Estornell, et al., 2011) (Liu et al., 2007) (Liu, 2008).

LiDAR is a remote sensing technique that allows to determine the distance to an object or surface using a laser pulse (Attila and Hajnalka, 2015). This technology provides digital models of the terrain with higher resolution than traditional methodologies, as it acquires dense point clouds capable of returning the smallest morphological variations (Meng et al., 2010).

Three main problems afflict the determination of the accuracy of the results in the comparative analysis of alternative methods: the possible different meaning of coastline relative to the operational context, the measurement of the results accuracy, and the appropriateness of the comparison element. As far as the first aspect is concerned, in the remotely sensed image we see the instantaneous coastline (Modava et al., 2019) which depends on the date and time of the data acquisition as it is linked to the tides and sea weather conditions (Aguilar et al., 2010). To measure the accuracy of the result, it is necessary to choose an indicator able to best express the difference between the coastline obtained and that of comparison. Finally, the element used as reference must be coeval with the image as we cannot

* Corresponding author

compare different temporal situations. The sources to be compared can refer to different and distant dates only if it is certain that no changes have occurred on the stretch of coast in the elapsed time interval.

This article aims to identify an effective methodological approach to compare different methods for detecting the coastline in Sentinel-2 multispectral images. The attention focuses only on easily applicable algorithms for coastline extraction without using training sites; in other terms, the unsupervised approach applied to maps resulting from the usage of some indices is preferred. Finally, six different classification methods for coastline identification based on the following indices are considered: Normalized Difference Vegetation Index (NDVI), Normalized Difference Water Index (NDWI), Modified Normalized Difference Water Index (MNDWI), Enhanced Vegetation Index (EVI), Red-Green Ratio (RGR) and NIR-Red Ratio (NRR). In all cases we use k-Means algorithm to classify each index resulting product in two clusters, i.e. water and no-water. The automatic vectorization allows to detect the coastline as separation between land and sea. To define the accuracy level of the results, two different coastlines are introduced as reference both in vector format: the coastline obtained from the DEM produced with 3D LiDAR data and presenting cell size 2 m x 2 m, and the manually vectorised one based on RGB photointerpretation.

2. STUDY AREA AND DATASET

The experiments are carried out on Sentinel-2A imagery, acquired on 6 August 2019, presenting a 2A processing level, concerning a part of the metropolitan city of Naples (Italy) as shown in Figure 1.

In particular, we examine the stretch of coast belonging to Torre Annunziata and Castellammare di Stabia (towns overlooking the Gulf of Naples), so to have a very varied scenario of the Campania Coastal morphology (Budillon et al., 2020), including anthropic constructions such as ports, and natural elements such as sandy and low-sloping beaches in the north and central parts, and high cliffs in the southernmost zone.

The used DEM is supplied by Italian Ministry for the environment (Ministero dell'Ambiente) and it is obtained from LiDAR data, acquired in 2008, characterized by a density of survey points greater than 1.5 points per square meter. The LiDAR generated DEM (Lg-DEM) has a vertical accuracy of less than ± 15 cm, while the horizontal accuracy is ± 30 cm. Figure 2 shows the 3D photorealistic model of the study area resulting from drapery of the Sentinel-2 RGB true colour composition on the Lg-DEM.

The Lg-DEM in the considered area also has negative values: these are representative of the seabed below the coast. Therefore, the reference coastline is extracted as the contour line at zero elevation from the Lg-DEM. Note that this is referred to the Italian vertical datum (EPSG:1051) that is determined by the mean sea level estimated at tide gauge station of Genoa (44°24'43.3" N, 08°55'32.2" E) managed by the Italian Hydrographic Institute.

Sentinel-2 images can be downloaded for free from the Copernicus platform, managed by the European Space Agency (ESA) (Copernicus Open Access Hub, 2022). Two satellites make up the Sentinel-2 constellation, named Sentinel-2A and Sentinel-2B. Sentinel-2B images are used for this study, the characteristics of which are shown in Table 1 (Sentinel-2 User Handbook, 2015).

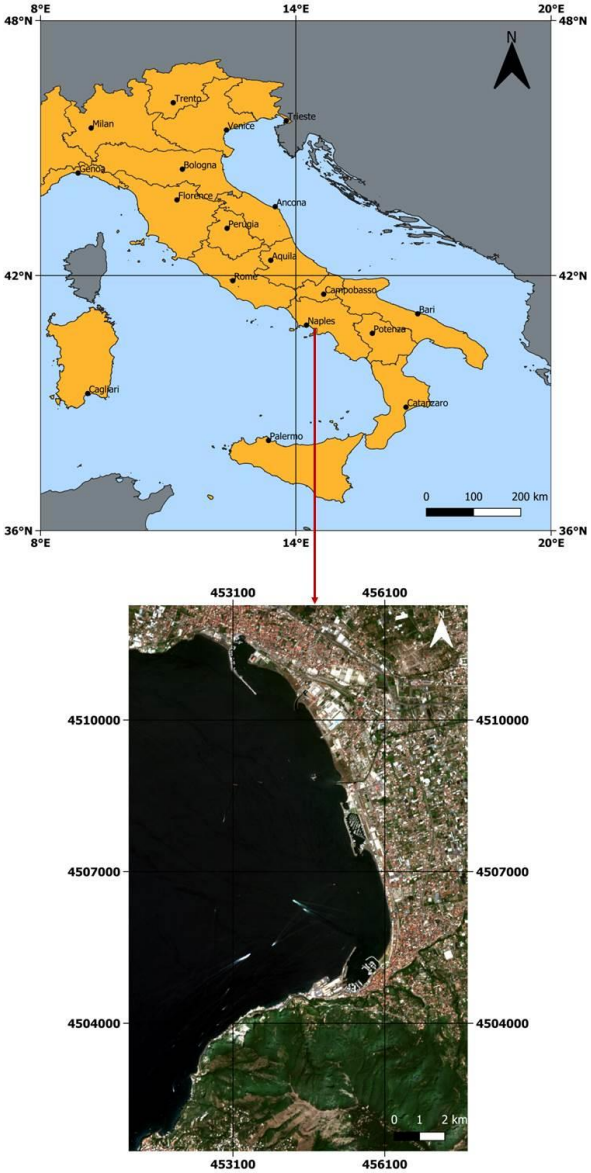

Figure 1. The study area: upper, localization of the study area in equirectangular projection and WGS84 geographic coordinates (EPSG: 4326); lower, visualization in RGB composition of Sentinel-2 images in UTM/WGS 84 plane coordinates expressed in meters (EPSG: 32632).

Figure 2. 3D photorealistic model of the study area resulting from drapery of the Sentinel-2 RGB true colour composition on the Lg-DEM.

Bands	Central Wavelength (nm)	Resolution (m)
B1 – Coastal	443	60
B2 – Blue	490	10
B3 – Green	560	10
B4 – Red	665	10
B5 – Red Edge	705	20
B6 – Red Edge	740	20
B7 – Red Edge	783	20
B8 – NIR	842	10
B8A – NIR	865	20
B9 – Vapour	945	60
B10 – SWIR	1375	60
B11 – SWIR	1610	20
B12 – SWIR	2190	20

Table 1. Main characteristics of Sentinell-2A images.

The study area extends between the following UTM/WGS84 zone 33N coordinates: E_1= 451,040 m; E_2= 457,740 m; N_1= 4,501,470 m; N_2= 4,512,270 m. The total covered surface is equal to 72.36 Km^2, and each image has a 670x1080 pixels format.

3. METHODS

3.1 Index Calculation

In this section we present the six indices used for the experiments, reporting formulas and a brief description of the main characteristics of each of them.
Normalized Difference Vegetation Index (NDVI) is an indicator that allows to highlight the presence of vegetation on satellite image, exploiting the peculiarity of the spectral signature of the vegetation that is characterized by low reflectance in red band and high reflectance in near infrared (NIR) band (Rouse et al., 1974). It allows to distinguish also the classes of water and bare soil (Alcaras et al., 2019). It is obtained by applying the following formula:

$$NDVI = \frac{NIR - Red}{NIR + Red} \quad (1)$$

However, one of the most largely used index for coastline detection in remotely sensed is Normalized Difference Water Index (NDWI). This index is proposed by McFeeters (McFeeters, 1996). Using two bands, Green and NIR, it allows to enhance the presence of the water in a remotely sensed image and can be obtained as follow:

$$NDWI = \frac{Green - NIR}{Green + NIR} \quad (2)$$

Figure 3 shows the output obtained by the application of NDWI to the Sentinel Green (B3) and NIR (B8) bands.

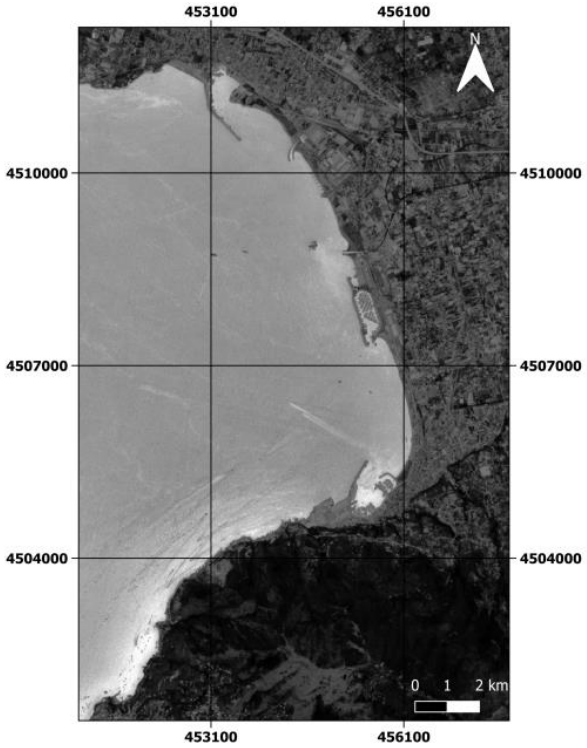

Figure 3. NDWI obtained from the Sentinel-2A images in UTM/WGS 84 plane coordinates (EPSG: 32633).

Modified Normalized Difference Water Index (MNDWI) was proposed by Wei et al. (Wei et al., 2011), it is generally used for urban areas. In fact, it permits to enhance and extract information on water as this index allows to reduce the noise generated by the buildings. The formula is shown below:

$$MNDWI = \frac{Blue - NIR}{Blue + NIR} \quad (3)$$

These first three indices can assume values in the range [-1, 1]. In particular, while in the NDVI the lowest values are representative of water, in the NDWI and in the MNDWI the highest values are representative of water.
The enhanced vegetation index (EVI) is an 'optimized' vegetation index that provides improved sensitivity in high biomass regions while minimizing soil and atmosphere influences. EVI is calculated in this way (Huete et al., 2002):

$$EVI = 2.5 \cdot \frac{NIR - RED}{NIR + 6 \cdot RED - 7.5 \cdot BLUE + 1} \quad (4)$$

The last two indices used are Red-Green Ratio (RGR) index and NIR-RED Ratio (NRR) index (Lacaux et al., 2007):

$$RGR = \frac{Red}{Green} \quad (5)$$

$$NRR = \frac{NIR}{Red} \quad (6)$$

As for the NDVI, in these last three indices the water assumes the lowest values.

3.2 K-Means Clustering

K-Means clustering is applied to each index, extracting two clusters (water/no-water) in order to classify the images. This procedure is carried out in SAGA GIS (Version 2.3.2) (Conrad et al., 2015). K-means is a numerical, unsupervised, non-deterministic, iterative method usable for image classification (Ahmed et al., 2020).
The central idea of this algorithm is to fix a priori the number of clusters k and to iteratively modify the partition, assigning each element x to the relative cluster, with the nearest mean, and then to recalculate the position of the average itself, as long as it remains unchanged (MacKay, 2003).
Hence, the K-Means algorithm attempts to locate the vector of means (μ_i) in the multidimensional spectral space (i.e. in the l bands) for each of the k classes (i.e. per i = 1, 2, …, k). Initially, the localization estimates of the vectors of the means are chosen at random (Nazeer and Sebastian, 2009).
If we indicate these initial estimates with μ''_i, it is possible to tentatively assign each pixel to a class based on a criterion of minimum distance from the mean, that is, how close that pixel is to each "vector of means" relating to each hypothetical class (Sinaga and Yang, 2020). The average of all the pixels tentatively assigned to the i-th class becomes our new estimate μ'_i of that class (Alcaras et al., 2021b).
With respect to the latter, the pixels are reassigned using the same minimum distance criterion and the procedure is repeated until no significant variation in the averages is observed.
However, in this case, the two resulting clusters effectively correspond to the researched classes: water/no water. The result of K-Means clustering applied to NDWI is shown in Figure 4.
From each thematic map, the coastline is automatically extracted in vector format as polyline separating pixels classified as water from pixels classified as no-water.

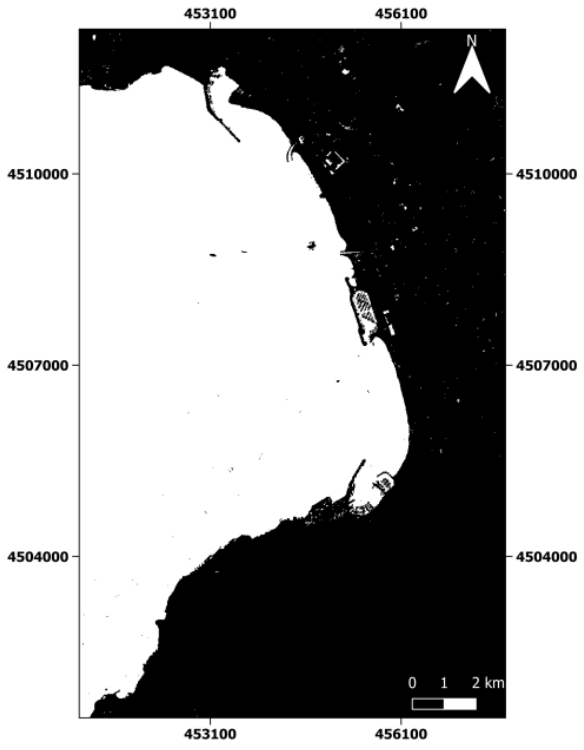

Figure 4. Result of K-Means clustering applied to NDWI: land is represented in black, while water is represented in white.

3.3 Accuracy Assessment

In order to evaluate the effectiveness of the applied methods, an accuracy assessment must be carried out. Generally, the obtained coastline is compared with another reference coastline, both in vector format. The latter can be achieved from the RGB composition or the panchromatic image (if available) of the same dataset (Maglione et al., 2015), from higher resolution images (Costantino et al., 2020), or from other sources.
In this study we want to explore the possibility of carrying out accuracy tests using the coastline automatically extracted from Lg-DEM. Giving the variability of elevation as well as depths near the coast, Lg-DEM allows to easily identify the separation between land and sea as the line dividing positive from negative height values. However, the use of the Lg-DEM to extract the reference coastline presents some criticalities highlighted below.
1. The first is closely linked to the definition of the coastline itself, as a matter of fact this can be considered as the instantaneous coastline, which is the one photographed at a specific time (Modava et al., 2019), or the coastline corrected by tidal effects and sea water conditions (Aguilar et al., 2010). In the case examined in this work we can say that the two coastlines are not distinguishable due to the resolution of the images (10 m) which does not allow to appreciate the differences between high and low tide.
2. Like in any other research field, it is often essential to associate
multispectral images, with LiDAR data acquired at the same time (Chouari, 2021). The coastline may in fact be affected by erosion or nourishment. In this study the acquisition times of the two data are very distant (2008 for the LiDAR survey and 2019 for the satellite image) and for this reason only the stretches of coast that have not changed over time are considered, which are equal to 55.16% of the total length of the coast.
3. The accuracy of the Lg-DEM and remotely sensed images must be comparable. Usually LiDAR data collected by sensor on airplane are referenced to the ground using kinematic differential global positioning system (GPS) methods, providing vertical accuracy to within few centimetres (Brock and Sallenger, 2001). Small laser spot size and high pulse frequency results in DEM products being produced at a very high resolution, e.g. 1-m resolution or higher (Nayegandhi and Brock, 2002). In our study, the Sentinel pixel dimensions are 10 m x 10 m while the Lg-DEM resolution is 2 m x 2 m. Despite the difference in size, the comparison is possible, given the high accuracy of the coastline obtained from the Lg-DEM.
Two indices present in literature are applied for testing the accuracy of the resulting coastline in vector format: the Ratio Index (RI) introduced in Maglione et al. (Maglione et al., 2014), and the Distributed Ratio Index (DRI) developed by Alcaras et al. (Alcaras et al., 2022). The first index allows to define the mean deviation of the extracted coastline from the reference one and is expressed in meters. The second index calculates RI for each of the polygons generated by the intersection between the reference coastline and each of the extracted ones, so it is more suitable for the analysis of the level accuracy of the results.
Particularly, if the overlap between the two lines does not occur perfectly, polygons are generated: considering their area (A), and the length of the reference coastline (L), RI is defined as follow:

$$RI = \frac{A}{L} \tag{7}$$

DRI works similarly to RI, considering every polygon that is generated between the two coastlines, so as to provide all possible statistical values (min, max, mean, standard deviation

and RMSE) for the deviation between the two examined coastline.
The pixel size is used as the spatial unit for the accuracy assessment (Stehman and Wickham, 2011).
In other words, to evaluate the effectiveness of the results, we analyse the coastline detectable in automatic way as vector feature in each resulting thematic map as separation between water and no-water, and consider its deviations from the reference one that is the Lg-DEM coastline.

4. RESULTS AND DISCUSSION

The tables reported in the first part of this section, (Tables 2 and 3) show the values of the indices used for the accuracy test conducted in this study and based on the reference coastline extracted from Lg-DEM.

Method	RI (m)
NDVI	8.56
NDWI	6.40
MNDWI	7.28
EVI	8.67
RGR	7.90
NRR	8.68

Table 2. RI values for the extracted coastlines using coastline extracted from Lg-DEM as reference.

Method	Mean (m)	St. Dev. (m)	RMSE (m)	Min (m)	Max (m)
NDVI	4.20	5.31	6.77	0.01	58.60
NDWI	2.71	2.84	3.92	0	19.26
MNDWI	2.71	3.03	4.06	0	19.16
EVI	3.56	3.83	5.23	0.02	24.48
RGR	3.00	4.05	5.04	0.01	43.28
NRR	3.72	4.83	6.10	0.02	51.23

Table 3. DRI statistical values for the extracted coastlines using coastline extracted from Lg-DEM as reference.

The values shown in Table 2 demonstrate that the best results are achieved by applying the K-Means on NDWI (6.40 m), while EVI and NRR present the worst results (8.67 m and 8.68 m respectively), although they turn out to be appreciable results as they are all below the pixel size.
Analysing the RMSE values in Table 3, also in this case, the K-Means applied on the NDWI provides the best results, while the worst output is achieved by the NDVI.
The experiments confirm the good performance of the NDWI submitted to K-Means algorithm. All indices supply the average value of the deviation less than the pixel size, but in the case of NDVI, NRR and RGR the maximum values are very high (58.60 m, 51.23 m and 43.28 m respectively).
The tables reported below (Tables 4 and 5) show the results obtained, in terms of RI and DRI, using the manually vectorised coastline as a reference term. The resulting values are comparable with those reported in Tables 2 and 3 referred to the coastline extracted from Lg-DEM.

Method	RI (m)
NDVI	9.98
NDWI	7.04
MNDWI	7.95
EVI	10.00
RGR	8.81
NRR	10.05

Table 4. RI values for the extracted coastlines using manually achieved coastline (based on visual interpretation of RGB composition) as reference.

Method	Mean (m)	St. Dev. (m)	RMSE (m)	Min (m)	Max (m)
NDVI	6.26	6.89	9.31	0.01	50.40
NDWI	4.42	3.60	5.70	0.03	26.65
MNDWI	5.06	4.33	6.65	0.03	26.57
EVI	5.77	4.99	7.62	0.01	27.52
RGR	4.83	5.26	7.15	0.00	53.09
NRR	5.93	6.16	8.55	0.01	52.94

Table 5. DRI statistical values for the extracted coastlines using manually achieved coastline (based on visual interpretation of RGB composition) as reference.

Also in this case the results obtained, both as regards the RI and the DRI, remark the optimal performance of the combination between the K-Means and the NDWI.
Particularly, analysing the values reported in table 4, it is possible to note that, also in this case, the EVI and the NRR present the worst results in terms of RI.
As regards the results shown in table 5, comparable with those shown in table 3, it can be noted that, by analysing the RMSE, the NDWI with the K-Means generates the best result, while the NDVI gives the worst result.
The manually achieved coastline from RGB composition is 78.05% shorter than the one obtained from the Lg-DEM. This factor affects the results, in fact, by analysing Tables 4 and 5 you can see that all the values have increased if compared to the corresponding ones in Tables 2 and 3. You can also note how the order of effectiveness of each method, identified by the RI in Tables 2 and 4, and by the RMSE in Tables 3 and 5, remain unchanged. Furthermore, the results obtained using the coastline derived from Lg-DEM as reference term are the best ones: this can be attributed not only to the human error that afflicts the manual vectorization, but also to the different geometric resolution of the two datasets, the Lg-DEM at 2 m x 2 m and Sentinel-2 RGB image at 10 m x 10 m.

5. CONCLUSIONS

This study demonstrates that the coastline derived from Lg-DEM can be assumed as reference term to compare various methods applicable for coastline extraction from remotely sensed images. Since the extraction of the coastline from a Lg-DEM is a very fast operation, we can avoid consuming the time of manual photointerpretation and vectorization starting from the remotely sensed images in RGB composition.
To achieve valid results, at least three aspects need careful evaluation. First of all, due to the dynamic nature of the coastline and the territorial transformations caused by natural and anthropogenic factors, the Lg-DEM and satellite images must be contemporary or, if acquired at different times, cover an area which, in the time interval elapsed, has not undergone any changes. Since the instantaneous coastline is extracted from the images and the coastline relative to the vertical datum from the

Lg-DEM, this difference must be taken into account, e.g. evaluating the tide value at the date and time of the image acquisition. An accurate coastline is necessary as reference; a Lg-DEM with pixel dimensions shorter than those of satellite images is to prefer.
Finally, we want to remark that the application of K-Means on NDWI is a very performing approach to distinguish water pixel from no-water ones on Sentinel-2 images, so to detect the coastline accurately (RMSE is much less than the pixel size).

REFERENCES

Aguilar, F.J., Fernández, I., Pérez, J.L., López, A., Aguilar, M.A., Mozas, A., Cardenal, J., 2010: Preliminary results on high accuracy estimation of shoreline change rate based on coastal elevation models. *Int. Arch. Photogramm. Remote Sens. Spatial Inf. Sci.*, 33 (8), 986-991.

Ahmed, M., Seraj, R., Islam, S. M. S., 2020: The k-means algorithm: A comprehensive survey and performance evaluation. *Electronics*, 9(8), 1295. https://doi.org/10.3390/electronics9081295.

Alcaras, E., Errico, A., Falchi, U., Parente, C., Vallario, A., 2019: Coastline extraction from optical satellite imagery and accuracy evaluation. In *International Workshop on R3 in Geomatics: Research, Results and Review*, 336-349. Springer, Cham. https://doi.org/10.1007/978-3-030-62800-0_26.

Alcaras, E., Amoroso, P. P., Baiocchi, V., Falchi, U., Parente, C., 2021a: Unsupervised classification based approach for coastline extraction from Sentinel-2 imagery. In *2021 International Workshop on Metrology for the Sea; Learning to Measure Sea Health Parameters (MetroSea)*, 423-427. IEEE. https://doi.org/10.1109/MetroSea52177.2021.9611583.

Alcaras, E., Amoroso, P. P., Parente, C., Prezioso, G., 2021b: Remotely Sensed Image Fast Classification and Smart Thematic Map Production. *ISPRS-International Archives of the Photogrammetry, Remote Sensing and Spatial Information Sciences*, *46*, 43-50. https://doi.org/10.5194/isprs-archives-XLVI-4-W5-2021-43-2021.

Alcaras, E., Falchi, U., Parente, C., Vallario, A., 2022: Accuracy evaluation for coastline extraction from Pléiades imagery based on NDWI and IHS pan-sharpening application. *Applied Geomatics*, 1-11. https://doi.org/10.1007/s12518-021-00411-1.

Attila, J., Hajnalka, N., 2015: Detecting military historical objects by LiDAR data. *AARMS–Academic and Applied Research in Military and Public Management Science*, 14(2), 219-236. https://doi.org/10.32565/aarms.2015.2.8.

Bo, G., Delleplane, S., De Laurentiis, R., 2001: Coastline extraction in remotely sensed images by means of texture features analysis. In *IGARSS 2001, Scanning the Present and Resolving the Future. Proceedings. IEEE 2001 International Geoscience and Remote Sensing Symposium* (Cat. No. 01CH37217), 3, 1493-1495. IEEE. https://doi.org/10.1109/IGARSS.2001.976889.

Budillon, F., Amodio, S., Contestabile, P., Alberico, I., Innangi, S., Molisso, F., 2020: The present-day nearshore submarine depositional terraces off the Campania coast (South-eastern Tyrrhenian Sea): an analysis of their morpho-bathymetric variability. *MetroSea 2020 - TC19 International Workshop on Metrology for the Sea, 2020*, 132-138.

Brock, J., Sallenger, A. H., 2001: Airborne topographic LiDAR mapping for coastal science and resource management. *US Geological Survey*, Center for Coastal Geology, 2001(46). https://doi.org/10.3133/ofr0146.

Chen, Z., Gao, B., Devereux, B., 2017: State-of-the-art: DTM generation using airborne LIDAR data. *Sensors*, 17(1), 150. https://doi.org/10.3390/s17010150.

Chouari, W., 2021: Contributions of multispectral images to the study of land cover in wet depressions of eastern Tunisia. *The Egyptian Journal of Remote Sensing and Space Science*, 24(3), 443-451. https://doi.org/10.1016/j.ejrs.2020.11.003.

Conrad, O., Bechtel, B., Bock, M., Dietrich, H., Fischer, E., Gerlitz, L., Wehberg, J., Wichmann, V., Böhner, J., 2015: System for Automated Geoscientific Analyses (SAGA) v. 2.1.4, *Geosci. Model Dev*., 8, 1991-2007. https://doi.org/10.5194/gmd-8-1991-2015.

Copernicus Open Access Hub, 2022. https://scihub.copernicus.eu/ (Accessed on 05/04/2022).

Costantino, D., Pepe, M., Dardanelli, G., Baiocchi, V., 2020: Using optical Satellite and aerial imagery for automatic coastline mapping. *Geographia Technica*, 15(2), 171-190. http://dx.doi.org/10.21163/GT_2020.152.17.

Darwish, K., Smith, S. E., Torab, M., Monsef, H., Hussein, O., 2017: Geomorphological changes along the Nile Delta coastline between 1945 and 2015 detected using satellite remote sensing and GIS. *Journal of Coastal Research*, 33(4), 786-794. https://doi.org/10.2112/JCOASTRES-D-16-00056.1.

Dolan, R., Hayden, B.P., May, P., May, S., 1980: The reliability of shoreline change measurements from aerial photographs. *Shore and beach*, 48(4), 22-29.

Estornell, J., Ruiz, L. A., Velázquez-Martí, B., Hermosilla, T., 2011: Analysis of the factors affecting LiDAR DTM accuracy in a steep shrub area. *International Journal of Digital Earth*, 4(6), 521-538. https://doi.org/10.1080/17538947.2010.533201.

Fabris, M., 2021: Monitoring the Coastal Changes of the Po River Delta (Northern Italy) since 1911 Using Archival Cartography, Multi-Temporal Aerial Photogrammetry and LiDAR Data: Implications for Coastline Changes in 2100 AD. *Remote Sensing*, 13(3), 529. https://doi.org/10.3390/rs13030529.

Goksel, C., Senel, G., Dogru, A. O., 2019: Determination of shoreline change along the Black Sea coast of Istanbul using remote sensing and GIS technology. *Desalination and Water Treatment*, *177*, 242-247. https://doi.org/10.5004/dwt.2020.24975.

Huete, A., Didan, K., Miura, T., Rodriguez, E. P., Gao, X. Ferreira, L. G., 2002: Overview of the radiometric and biophysical performance of the MODIS vegetation indices, *Remote sensing of environment*, vol. 83.1-2, 195-213. https://doi.org/10.1016/S0034-4257(02)00096-2.

Karaman, M., 2021: Comparison of thresholding methods for shoreline extraction from Sentinel-2 and Landsat-8 imagery: Extreme Lake Salda, track of Mars on Earth. *Journal of*

Environmental Management, 298, 113481. https://doi.org/10.1016/j.jenvman.2021.113481.

Lacaux, J. P., Tourre, Y. M., Vignolles, C., Ndione, J. A., Lafaye, M., 2007: Classification of ponds from high-spatial resolution remote sensing: Application to Rift Valley Fever epidemics in Senegal. *Remote Sensing of Environment*, vol. 106.1, 66-74. https://doi.org/10.1016/j.rse.2006.07.012.

Liu, X., Zhang, Z., Peterson, J., Chandra, S., 2007: The effect of LiDAR data density on DEM accuracy. In *Proceedings of the International Congress on Modelling and Simulation* (MODSIM07), 1363-1369. Modelling and Simulation Society of Australia and New Zealand Inc.

Liu, X., 2008: Airborne LiDAR for DEM generation: some critical issues. *Progress in physical geography*, 32(1), 31-49. https://doi.org/10.1177/0309133308089496.

Liu, Y., Wang, X., Ling, F., Xu, S., Wang, C., 2017: Analysis of coastline extraction from Landsat-8 OLI imagery. *Water*, 9(11), 816. https://doi.org/10.3390/w9110816.

MacKay, D., 2003: An example inference task: Clustering. *Information theory, inference and learning algorithms*, 20, 284-292.

Maglione, P., Parente, C., Vallario, A., 2014: Coastline extraction using high resolution WorldView-2 satellite imagery. *European Journal of Remote Sensing*. 47(1), 685-699. https://doi.org/10.5721/EuJRS20144739.

Maglione, P., Parente, C., Vallario, A., 2015: High resolution satellite images to reconstruct recent evolution of domitian coastline. *American Journal of Applied Sciences*, 12(7), 506. https://doi.org/10.3844/ajassp.2015.506.515.

McFeeters, S. K., 1996: The use of the Normalized Difference Water Index (NDWI) in the delineation of open water features. *International journal of remote sensing*, 17(7), 1425-1432. https://doi.org/10.1080/01431169608948714.

Meng, X., Currit, N., Zhao, K., 2010: Ground filtering algorithms for airborne LiDAR data: A review of critical issues. *Remote Sensing*, *2*(3), 833-860. https://doi.org/10.3390/rs2030833.

Modava, M., Akbarizadeh, G., Soroosh, M., 2019: Hierarchical coastline detection in SAR images based on spectral-textural features and global–local information. *IET Radar Sonar Navig*, 13(12), 2183-2195. https://doi.org/10.1049/iet-rsn.2019.0063.

Nahon, A., Molina, P., Blázquez, M., Simeon, J., Capo, S., Ferrero, C., 2019: Corridor mapping of sandy coastal foredunes with UAS photogrammetry and mobile laser scanning. *Remote Sensing*, 11(11), 1352. https://doi.org/10.3390/rs11111352.

Nayegandhi, A., Brock, J., 2002: Gridding NASA ATM coastal LiDAR data, in *Proceedings of the Seventh International Conference on Remote Sensing for Marine and Coastal Environments*, Miami, 20-22, May 2002.

Nazeer, K.A.A., Sebastian, M.P., 2009: Improving the Accuracy and Efficiency of the k-means Clustering Algorithm. In *Proceeding of the World Congress on Engineering*, Vol. 1, July 1 - 3, 2009, London, U.K.

Palazzo, F., Latini, D., Baiocchi, V., Del Frate, F., Giannone, F., Dominici, D., Remondiere, S., 2012: An application of COSMO-Sky Med to coastal erosion studies. *European Journal of Remote Sensing*, *45*(1), 361-370. https://doi.org/10.5721/EuJRS20124531.

Pawluszek-Filipiak, K., Borkowski, A., 2020: On the importance of train–test split ratio of datasets in automatic landslide detection by supervised classification. *Remote Sensing*, 12(18), 3054. https://doi.org/10.3390/rs12183054.

Prasad, D. H., Kumar, N. D., 2014: Coastal erosion studies—a review. *International Journal of Geosciences*, 2014, 5(4). https://doi.org/10.4236/ijg.2014.53033.

Rouse, J. W., Haas, R. H., Schell, J. A., Deering, D. W., 1974: Monitoring vegetation systems in the Great Plains with ERTS. *NASA special publication* 1974, 351, 309.

Sentinel-2 User Handbook, ESA, 2015. https://sentinels.copernicus.eu/documents/247904/685211/Sentinel2_User_Handbook (Accessed on 05/04/2022).

Sinaga, K. P., Yang, M. S., 2020: Unsupervised K-means clustering algorithm. *IEEE Access*, Vol. 8, 80716-80727. https://doi.org/10.1109/ACCESS.2020.2988796.

Sisodia, P. S., Tiwari, V., Kumar, A., 2014: Analysis of supervised maximum likelihood classification for remote sensing image. In *International Conference on Recent Advances and Innovations in Engineering* (ICRAIE-2014), 1-4. IEEE. https://doi.org/10.1109/ICRAIE.2014.6909319.

Specht, M., Specht, C., Lewicka, O., Makar, A., Burdziakowski, P., Dąbrowski, P., 2020: Study on the Coastline Evolution in Sopot (2008–2018) Based on Landsat Satellite Imagery. *Journal of Marine Science and Engineering*, *8*(6), 464. https://doi.org/10.3390/jmse8060464.

Stehman, S. V., Wickham, J. D., 2011: Pixels, blocks of pixels, and polygons: Choosing a spatial unit for thematic accuracy assessment. *Remote Sensing of Environment*, vol. 115.12, 3044-3055. https://doi.org/10.1016/j.rse.2011.06.007.

Viana, R. D., dos Reis, G. N. L., Velame, V. M. G., Körting, T. S., 2019: Shoreline extraction using unsupervised classification on Sentinel-2 imagery. In *Proceedings of XIX Brazilian Symposium on Remote Sensing*, Vol. 19.

Wei, Q., Jingxuan, L., Lin, L. I., Xiao-Wen, L., 2011: Research on automatic extraction of water bodies and wetlands on HJ satellite CCD images. *Remote Sensing Information*, 4, 28-33.